I.O.S.

A STRAIN GAUGE PRESSURE SENSOR FOR MEASURING TIDES ON THE CONTINENTAL SHELF

by

T.J.P. GWILLIAM AND P.G. COLLAR

REPORT NO.14

1974

NATURAL ENVIRONMENT RESEARCH COUNCIL

INSTITUTE OF OCEANOGRAPHIC SCIENCES

A STRAIN GAUGE PRESSURE SENSOR FOR MEASURING TIDES ON THE CONTINENTAL SHELF

by

T.J.P. GWILLIAM and P.G. COLLAR

REPORT NO. 14

1974

Institute of Oceanographic Sciences
Wormley
Nr. Godalming
Surrey
GU8 5UB

CONTENTS

LIST OF ILLUSTRATIONS

1. ABSTRACT

This report describes some work carried out, principally in 1971 and 1972, on the adaptation of a commercial strain gauge to the measurement of tides near the edge of the Continental Shelf. The composite sensor so produced is not without its limitations, but on the whole it can produce very acceptable open sea tide records. The circuit technique employed is certainly not new, but it has wider applications and in a number of instances where it could be used it seems to have been overlooked. For this reason it seemed appropriate to report on the work and on some of the limitations that have been encountered.

2. INTRODUCTION

For several years now the Institute of Oceanographic Sciences has been engaged on a series of open-sea tide measurements round the Continental Shelf edge conducted in support of its research programme on tides. The technique used - the only viable one in remote open sea locations - is to place a retrievable instrument on the seabed to record changes in pressure. If the information is required in terms of water level, rather than pressure, changes, these can be deduced subsequently provided that there is adequate knowledge both of the density through the water column and of changes in atmospheric pressure.

In measuring sea bed pressure a fundamental question arises of whether one measures absolute pressure, ie. against vacuum, or attempts to measure the changes against a reference pressure adjusted to mean conditions. In the first case a relatively high degree of stability is required of the sensor, both against temperature changes and with respect to time. (Typically we have encountered temperature fluctuations of $\lesssim 1^{\circ}C$ when attempting to measure a tidal change of 0.1-0.3 bars in an ambient of 10-20 bars). In the latter case the restraints imposed on the transducer are much reduced, but the problem of maintaining a stable reference is introduced. A simple calculation shows that at an ambient of 20 bars a change in temperature of the reference pressure chamber of $1^{\circ}C$ will produce an apparent pressure change of 70 m bars. This is particularly serious if, as often happens, temperature fluctuations are of tidal periodicity. We have a preference for measurement of absolute pressure, although sensors based on the second method do exist.

The accuracy required in measurement of tide pressure changes really depends on the use to which the data are to be put. In the present case the broad objective was to achieve a performance comparable to, or better than, that of a good, shore based stilling well gauge: measurement to well within 1% of the tidal range and freedom from instrumental distortion of the tide

record. This is important at the higher tidal frequencies because spurious harmonics and cross modulation products of the major diurnal and semi diurnal tides can easily mask real changes, which are usually of relatively low amplitude. We were also concerned that the instrumentally generated 'noise' in the record should be less than that due to small fluctuations in pressure occurring naturally.

It is not intended to give in this report an analysis of the way in which instrumental characteristics (such as sensitivity to temperature change) can affect measurement accuracy. It is difficult to be specific because the relative importance of different responses is rather dependent on the area in which the sensor* is being used. However, we have tried to list those factors which could prove important, and to give details of laboratory measurements on the sensor in each case. Skinner and Rae[1] have reviewed factors affecting the accuracy of pressure measurements and have conducted a valuable series of comparative measurements on a number of different sensor types: the sensor discussed in this report is not, however, included in this survey.

In our early work on measuring open sea tides the NIO variable capacitance sensor, originally developed for wave recording, was used.[2] The output was in the form of a frequency analogue and this was counted over a fifteen minute period to assist in reducing unwanted fluctuations in the pressure record arising from waves. This sensor produced, and is still producing, some very acceptable tide records. In its existing form, however, it was felt to be rather sensitive to temperature changes, and also it exhibited a slow drift in output frequency when subjected to a steady pressure. The magnitude of the drift varied between 20 mbars and 200 mbars per month at a typical pressure corresponding to 150 metres depth. These drifts can be removed from the record during subsequent processing without any significant loss of accuracy, provided that they do not exceed a few tens of mbars, and provided that there is no interest in changes of periodicity longer than a few days. Nevertheless the situation was unsatisfactory, and, since the cause of instability was thought to lie in the mechanical arrangement of diaphragm and capacitance plates, a completely fresh approach seemed necessary.

---

*We define the sensor as a composite unit containing a transducer and associated electronics, which includes an interface to a recording tide gauge. The transducer is essentially a passive unit which converts a pressure change to a change in a measurable electrical parameter such as resistance or capacitance.

Two commercial sensors which were considered as alternatives were a prototype sensor using a quartz crystal, manufactured by Hewlett-Packard, and the Vibrotron. The former was basically a piezo electric resonator, cut in such a way to give a maximum pressure sensitivity and minimum temperature sensitivity, whose output was compared with that of a similar, but capped, resonator. It was designed for use primarily at the very high ambient pressures (up to 700 bars) and relatively low temperatures encountered on the deep ocean floor, and indeed has been very successfully employed in the Snodgrass deep sea tide capsule[3]. The technical specification was generally very good, the drift, in particular, being less than 4 mbars/month at high pressure. The temperature sensitivity, smallest near $0^{o}C$ but 30-40 mbar/^{o}C at 20 bars, $10^{o}C$, was thought to be less well suited to conditions on the European Shelf where, in addition, larger fluctuations in temperature are to be expected. Although the Hewlett-Packard sensor offered a considerable improvement in long term stability its relatively high cost (a factor of six greater than that of the existing sensor) was an overriding consideration and it was therefore not used.

In the Vibrotron, pressure varies the frequency of a tungsten wire vibrating in a magnetic field. The a.c. voltage induced is amplified and fed back in the sense required to maintain the wire in oscillation. The sensor has been used for a number of years for wave and deep sea tidal measurements, but its performance with regard to stability is inferior to that of the quartz sensor. It required less power ($\sim$ 39mW) than the quartz sensor, but apart from some increase in stability did not seem to offer sufficient improvement over the variable capacitance sensor to justify a somewhat greater cost. At this point in time, (late 1970) M.J. Tucker suggested the use of a strain gauge which, in view of the well established design and assembly techniques used in the manufacture, might enable better mechanical stability to be achieved in a relatively cheap sensor.

3. PRINCIPLE OF OPERATION

One of the more important characteristics of a tide pressure sensor is that it should have an output which, when integrated to reduce wave induced pressure fluctuations, permits a high degree of stability to be achieved. (The alternative to integration is rapid sampling, and subsequent filtering during computer processing, but this is not possible in a remote self recording instrument in view of data storage limitations). Most commercial pressure transducers are in the form of a d.c. operated Wheatstone bridge whose arms are strain sensitive elements. The amplified out of balance output is proportional to applied pressure. Unfortunately it is difficult to achieve stable integration of d.c. signals over a period of 15 minutes, and so an a.c. method was chosen for converting a resistance change to a change in frequency. The origin of the technique, in which the resistive strain gauge forms one of two frequency determining elements in a phase shift oscillator, is obscure but the first mention seems to have been by Stastny and Butts [4]. Subsequently Hamon and Brown [5] used the technique in sensors for a temperature - chlorinity - depth recorder, which became the fore-runner of the S.T.D. system in use today.

The principle is as follows and is illustrated in fig. 1.

A capacitor placed in parallel with one arm of the bridge produces a phase shift in the bridge output which can be made strongly dependent on small changes in the state of bridge balance. At balance the phase shift is nearly $\pi/2$. The bridge output is fed to a dispersive phase shift network whose amplified output drives the bridge. If no other phase shifts are present in the loop, and provided sufficient loop gain exists, the circuit oscillates at the frequency at which bridge and p.s.n. phases are equal and opposite. If the capacitor is placed across an arm whose resistance increases with increasing pressure, the phase angle of the bridge output relative to the input is:

$$\phi_B = \tan^{-1} \frac{2\omega R_B C_B (R_B - \Delta R_B)(R_B + \Delta R_B)^2}{-8 R_B^2 \Delta R_B + \omega^2 C_B^2 (R_B + \Delta R_B)^2 (R_B - \Delta R_B)^3}$$

$$= \tan^{-1} \frac{2\omega R_B C_B}{-8\frac{\Delta R_B}{R_B} + \omega^2 R_B^2 C_B^2} \quad \text{(to within about 0.4\%)} \qquad \ldots\ldots (1)$$

$$(\omega = 2\pi f)$$

The simplest form for the p.s.n. is given by two low pass RC stages (elements R_N, C_N) for which the phase angle is:

$$\phi_N = \tan^{-1} \frac{-3\omega R_N C_N}{1-\omega^2 R_N^2 C_N^2} \qquad \ldots\ldots (2)$$

Provided there are no other phase shifts within the loop,

$$\phi_B + \phi_N = 0$$

By summing (1) and (2), the frequency of oscillation may be expressed as:

$$f^2 = f_o^2 \left\{ 1 \pm 12 \frac{R_N C_N}{R_B C_B} \left(\frac{\Delta R_B}{R_B} \right) \right\} \qquad \ldots\ldots (3)$$

(where the sign is positive or negative depending whether the capacitor C_B is placed across an arm whose resistance increases or decreases with increasing pressure.)

and f_o, the frequency at balance

$$= \frac{1}{2\pi} \sqrt{\frac{2}{R_N C_N (3R_B C_B + 2R_N C_N)}} \qquad \ldots\ldots (4)$$

Since the maximum value of $\Delta R_B/R_B$ is 0.004, it is clear from Eqn.3 that $R_N C_N \gg R_B C_B$ if a wide frequency range is required. Eqn.4 then approximates to $f_o \simeq \frac{1}{2\pi R_N C_N}$ ..... (5)

In practice some unwanted phase shift always exists, and this causes a departure from the simple square root dependence of f on ΔR_B. It is not worth pursuing the expression further since the way in which unwanted phase shift might itself vary with frequency is unknown. However we have found one result useful in assessing the effect of stray impedances. At balance, if an unwanted phase shift, ϕ, is present, the frequency of oscillation is given by

$$f = \frac{6\phi R_N C_N + \sqrt{36\phi^2 R_N^2 C_N^2 + 8R_N C_N (2R_N C_N + 3R_B C_B)}}{4\pi R_N C_N (3R_B C_B + 2R_N C_N)} \qquad \ldots\ldots (6)$$

For small Ø this represents a shift from the ideal case of

$$\Delta f \simeq \frac{3}{4\pi R_N C_N} \cdot \emptyset + \frac{9}{8\pi R_N C_N} \cdot \emptyset^2$$

ie. $\frac{\Delta f}{f_o} \simeq \frac{3}{2} \emptyset$. from Eqn. 5. ..... (7)

4. SPECIFICATION

In designing the oscillator circuit for the sensor the most fundamental decisions to be made concern the degree of linearity to be provided in converting pressure to frequency and whether compensation should be provided in situ for temperature sensitivity. Our inclination was to produce the simplest sensor we could devise since this seemed to be the best way to achieve the high stability, $\frac{\partial f}{\partial t}_{P,T}$, required, and to minimize development time and cost. There are few instances where oceanographic data are not processed in a computer and calibration non linearity and secondary sensitivities can be removed at this stage, following careful measurement in the laboratory.

One of the consequences of this approach is a spread in sensor characteristics over a batch. However since oceanographic instruments are, or should be, individually calibrated before and after use at sea this is not a drawback.

The main constraints on the design of the circuit were as follows:

1. A stability of 1 in 2.10^4 over one month in output frequency in order to achieve a stability in pressure measurement of this order. (1 mbar in 20 bars).
2. Power dissipation in the combined transducer and oscillator should not exceed 100 mW and preferably should be less.
3. The temperature coefficient (zero shift + slope change) of the sensor should not exceed 10 mbars /^{o}C at any pressure and should be stable.
4. The sensors should work satisfactorily between 0 and 30^{o}C and should be free from significant thermal hysteresis.
5. Operation over a wide range of supply voltages should be possible.
6. Changes in output frequency due to changes in supply voltages should be minimal.
7. The ratio of extreme frequencies (0 - 20 bar pressure change) should be about 2:1 to facilitate use with the tide gauge. The minimum output frequency should be at least 100 Hz.

8. If possible, integrated circuits should be used for active elements.
9. The sensor circuit should at least match the strain gauge transducer in overall performance (i.e. in terms of stability, temperature coefficient etc.).

5. DESIGN

5.1.1. Transducer

The most suitable transducer available at the time was found to be the Bell and Howell general purpose type 4-366. Pressure applied to the diaphragm is transmitted mechanically to a Wheatstone bridge which results in increased strain in two arms and reduced strain in adjacent arms.

The transducer was originally manufactured with a bridge impedance of 350 Ohms, but to meet the criterion of low power consumption this has since been increased to 1000 Ohms.

When testing the completed sensor it became apparent that the largest contribution to the overall temperature coefficient was that due to the strain gauge transducer. To compensate for this in the electronic circuits would, it was decided, introduce additional thermal lag. The strain gauge transducer is normally temperature compensated during manufacture by incorporating a small value resistance of correct coefficient in the bridge circuit and it was decided to retain this. A typical figure for the thermal zero and sensitivity shifts after compensation is of the order of 0.01%* F.R.O./^{o}C. Unfortunately, positioning the compensating resistors in the transducer housing still gives thermal lag problems: these are discussed in the later section on Secondary Characteristics.

The material used for the diaphragm and shell of the transducer is stainless steel (17-APH), which after several months immersion in sea water has shown no obvious signs of corrosion.

5.1.2. Amplifier

It was decided to base the circuit on the readily available SN72709 integrated operational amplifier, which at the time was the most suitable from the point of view of open loop gain, bandwidth, current drain, and input and output impedances. A balanced feed to the bridge was obtained by using a transformer. Circuit values were chosen to give an operating range of

*Full range output

~ 1000 to 2000 Hz as this is about mid-range for small audio frequency transformers. Phase shifts should therefore be minimal and stray impedances should not prove troublesome at these frequencies. Some form of amplitude limiting is, of course, required in the oscillator loop. Thermistor, f.e.t. and diode devices were used as non linear resistors to control loop gain. All appeared to work satisfactorily, although the use of a thermistor increased power consumption somewhat. Finally diodes were chosen although they do contribute a small phase shift and are temperature sensitive. However, these effects are not too large and the method has the merit of simplicity. The diodes perform best as an a.g.c. device when operated on the lower non linear portion of their characteristic, i.e. just conducting. For this reason the circuit is arranged to give a positive rather than negative pressure/frequency slope. The increase in bridge output as the bridge is unbalanced is largely offset by increased attenuation in the low pass filter, and the working point of the diodes therefore changes relatively little over the operating pressure range.

The circuit shows some dependence of output frequency on amplifier gain. Typically an increase in gain of 1% produces a change in frequency of up to 1 Hz. The gain setting resistors must therefore be adequately stable.

Finally, two feedback loops were provided in the circuit. The inner loop improves stability but, in particular, reduces the amplifier output impedance to a reasonable value (about 4 ohms). The outer diode feedback loop includes the transformer and marginally improves the phase response. Figure (2) shows the circuit diagram of the oscillator together with the buffer amplifier (IC2). The buffer amplifier causes less than 0.1 Hz frequency change at 1 KHz, and selection of components for high stability is therefore unnecessary.

The stability of the circuit against parasitic oscillations has been found to be good, although some care is required in obtaining the correct amplifier high frequency response. The stability of the complete oscillator loop at other than the wanted frequency has been verified by breaking the loop and measuring the open loop response from below 1 Hz to 500 KHz.

5.1.3. R.C. Networks

In the absence of unwanted phase shifts, the temperature coefficient and stability of the oscillator are determined by R_B, C_B, R_N and C_N (Equations 3 to 5). Apart from the transducer compensation no attempt was made to balance positive and negative coefficients arising in different parts of the sensor.

Generally speaking, components with the highest long term stabilities also exhibit the lowest temperature coefficients, and, since oscillator stability is of paramount importance, it was decided to select components primarily for their stability. For these reasons, sintered silver mica capacitors were chosen for C_N and C_B. These have extremes in temperature coefficient of 30±30ppm/^{o}C and a loss angle ~ 0.001 radians at 1 KHz. Stability data are few, but it is generally acknowledged that silvered mica capacitors are the most stable available. (A histogram published by one manufacturer shows that 80% of a silvered mica capacitor population remain within 0.2% of initial capacitance value over a 10 year active life).

The choice of resistor for R_N is a little wider. Vishay Welwyn metal film resistors were chosen initially, these having a shelf stability of 25 ppm over 12 months and a typical temperature coefficient of ± 1 ppm over the range 0 to 60^{o}C. Since it is now known that instability in R_N is far from being the limiting factor in the overall stability, this choice could be relaxed to Precision Grade wirewound resistors.

Values of R_N, C_N and C_B are fixed by equations (4) and (5). Apart from stray capacitance appearing across the bridge arms the only unwanted impedance of consequence associated with the R.C. network is the input impedance of the amplifier. In the worst case (lowest open-loop amplifier R_{in}, lowest open-loop amplifier gain) this will present a shunt impedance of 1.5 Meg ohms across the low pass network. It can be shown that for an overall stability of 1 in 2.10^4 to be achieved in the output frequency a stability of order 1% is required in this impedance. An improvement of a factor 2 could be obtained here by using the SN 52709A, which has a higher minimum input impedance. To date all circuits have used the standard SN 72709.

5.1.4. Transformer

The equivalent circuit of the transformer is shown in Fig. 4a together with values of the parameters in one of the original designs.*

---

*Discontinuation of the manufacture of core stampings for this transformer subsequently entailed using a larger size. The transformer parameters have consequently changed somewhat and the working frequency range is not centrally placed in the transformer pass band. However, this does not significantly affect the conclusions of the following sections.

Since the interest is in minimising the larger phase shifts, the circuit may be simplified considerably as shown in Fig. 4b. In particular, the core loss conductance, G_p, and shunt winding capacitances are sufficiently small to neglect in the present case. The conductance, G_p, changes a phase term

$$\frac{R_W}{\omega L_p} \quad \text{to} \quad \frac{R_W}{\omega L_p + R_W \tan \delta}$$

(where $\tan \delta \sim \omega L_p G_p$, the core loss angle)

A crude measurement of loss at 1 KHz suggested an upper limit for tan δ of 2.75 : $R_W = 10\Omega$. $\omega L_p \geqslant 12000\Omega$.

The combined winding capacities ($C' \sim C_p + C_s$) likewise produce a phase term of order

$$\tan^{-1} \frac{\omega (L_\ell + C' R_\ell R_W)}{(R_\ell + R_W) - \omega^2 L_\ell C' R_\ell}$$

Given that $L_\ell \sim$ 1mH, $C' <$ 500pf and $R_W \sim 10\Omega$, $R_\ell \sim 10000\Omega$, neglect of C' is justified at 1 - 2 KHz.

The phase angle introduced by the transformer may then be written very approximately as:

$$\phi \sim \tan^{-1}\left(\frac{R_W}{\omega L_p} - \frac{\omega L_\ell}{n^2 R_\ell}\right)$$

Each of the variables R_W, L_p, L_ℓ are to some extent dependent on each other and on the geometry and composition of available cores and also on the winding. An additional constraint is imposed by stray capacity within the transformer, which can appear across the bridge arms. This can be minimised either by reducing the common surface area of the windings and (earthed) core, or by increasing the gap between them. The first solution effectively reduces L_p, the second increases L_ℓ and so a compromise must be sought.

The primary:secondary turns ratio, also, represents a compromise. If n is too low, additional phase shift arises because more gain is required from the amplifier. This in turn leads to problems with d.c. offset, typically a millivolt or two (referred to the input) for these circuits. If n is too high additional phase shift is incurred in the transformer. In practice the gain required to sustain oscillation is about 1000 and this can be supplied by one amplifier if the transformer turns ratio is near unity. An offset is present but the oscillator operates quite satisfactorily with ±7 volt supplies.

5.1.5. Diodes

The effects of the back to back diodes are complex. The equivalent circuit is a voltage dependent resistance shunted by diffusion (forward bias) and depletion (reverse bias) capacitances, both of which are also voltage dependent. However for practical purposes the diodes can be considered to act as a resistance of about 1 Meg ohm shunted by a capacitance of approximately 2 pf.

5.1.6. Stray impedances

Having attempted to minimise unwanted phase shifts in the design, an attempt was made to assess how successful this had been. It is not practicable to make direct measurements of small phase shifts, but estimates can be made by measuring accurately values of C_N, R_N, C_B, R_B and ΔR_B and comparing the predicted characteristic with that actually obtained.

In practice it proves easier to introduce a change ΔR_B in only one arm of the bridge rather than make equal changes in all four arms. In the absence of unwanted phase shifts elsewhere in the circuit, the frequency of oscillation is then given exactly by

$$f = \frac{1}{2\pi}\sqrt{\frac{6R_NC_N \cdot \Delta R_B + R_BC_B(2R_B + \Delta R_B)}{R_BC_BR_NC_N\,(3R_B^2C_B + R_NC_N(2R_B + \Delta R_B))}} \qquad \ldots\ldots(8)$$

for the case where arm 1 is increased by ΔR_B and the capacitor C_B shunts arm 3.

The measurements summarised in table I were carried out on an early prototype. Only the two extreme values of ΔR_B were selected because it was known that the $f^2 \propto \Delta R_B$ relationship holds fairly well overall. (Fig. 3).

R_B = 999.8 ± 0.01% ohms. C_N = 0.01500 ± 0.05% µf.

R_N = 10.000 ± 0.01% kilohms. C_B = 1990 ± 1 pf.

(Values of R_B, C_B, R_N, C_N, ΔR_B were selected by measurement from a stock of close tolerance components. Oscillators A,B,C were obtained by substituting three transformers, wound to the same nominal specification, into the same circuit in turn).

Oscillator	ΔR_B	Measured f	Calculated f	Apparent Phase error (rad)
1	0	1039	1050.6	0.008
1	15.03	2123	2197	0.023
2	0	1036	1050.6	0.010
2	15.03	2120	2197	0.024
3	0	1041	1050.6	0.007
3	15.03	2115	2197	0.025

Table I. Comparison of oscillation frequencies predicted by Eqn. 8. with those actually obtained

The results suggested that unwanted phase shifts approaching 0.01 rad. lag (1.05 KHz) and $\sim$ 0.025 rad. lag (2.2 KHz) were present in the loop. Neglecting capacitances, the average phase shifts calculated for these early transformers were 0.001 rad. lag at 1.05 KHz and 0.013 lag at the upper end of the frequency range. At the lower frequency ($\Delta R_B = 0$) we attribute most of the remaining 0.006 to 0.009 rad. phase angle to the combined effects of the amplifier, forward resistance and reverse bias capacitance of the limiting diodes. At the upper frequency, although this contribution is probably increased slightly, there is evidence that stray capacity, introduced mainly by the transformer, also plays a part. It effectively appears across one or other of the bridge arms and adds to or subtracts from C_B. To obtain an estimate the polarities of primary and secondary connections were reversed. A decrease in frequency of between 70 and 76 Hz was noted for each transformer at the upper end of the frequency range, with little change at the lower end. This can be accounted for by an unbalanced stray equivalent to $\sim$ 90 pf across C_B, producing a phase angle of 0.013 rad. An unorthodox winding procedure was evolved for later transformers to try to minimise stray capacitance.

6. SECONDARY CHARACTERISTICS

Although a sensor is designed to respond to a specific parameter, in this case pressure, it nevertheless invariably has some degree of unwanted sensitivity to secondary parameters such as temperature and time (stability). Instrumental parameters such as supply voltages may also be important. It is clearly essential to know how the sensor behaves in these respects and, in particular, what limitations such sensitivities may place on the use of the sensor and the data obtained from it.

A large number of measurements have been made in the laboratory of the characteristics of the pressure sensor and to complement these a study has been made of pressure records obtained in the open sea. The following sections describe some of these measurements. In the case of the temperature sensitivity we have tried to assess which parts of the sensor make the greatest contribution to the overall effect.

6.1. Temperature Coefficient

The temperature coefficient of the sensor at a given working pressure represents the sum of a number of contributions and an attempt has been made here to assess these individually.

6.1.1. Amplifier phase shift, input and output impedances

These are difficult to measure individually at other than room temperature. An approximate measure of their combined effect was obtained by cooling the amplifier in situ and looking for a change in output frequency. This was negligible.

6.1.2. Transformer

(a) Winding resistance R_W. The variation of the resistivity of copper with temperature should give an increase in frequency of $\sim$ 30 ppm/^{o}C at 1 KHz and a slightly smaller change at 2 KHz. This gives a contribution to $\left(\frac{\Delta P}{\Delta T}\right)_{P=O} \simeq 0.6$ mbs/^{o}C .

(b) Magnetising inductance, L_p. Depends on the way in which the core stampings are arranged. Measurements made on one transformer with a gapped core showed $< 2\%$ reduction in L_p over a 20^{o}C range. This would give a reduction in frequency $\sim$ 10 ppm/^{o}C i.e. a contribution to $\left(\frac{\Delta P}{\Delta T}\right)_{P=O} \sim$ -0.2 mbs/^{o}C.

(c) Leakage inductance, L_ℓ . Direct measurement showed $< 2\%$ change over a $20^{\circ}C$ range i.e. of the same order as that in L_p. This would give an increase in frequency of < 20 ppm/$^{\circ}C$. The effect would be greater at 2 KHz.

(d) Load resistance, R_L (= R_B). Direct measurement on a 1000Ω transducer showed a change in load of ~ 300 ppm/$^{\circ}C$. This would result in an increase in frequency of a few ppm/$^{\circ}C$ and the effect is virtually negligible.

6.1.3. Low pass filter

A small change in R_N, δR_N, produces a change in output frequency, δf such that

$$\frac{\delta f}{f} = \frac{-1}{2f^2} \cdot \frac{\delta R_N}{R_N} \left\{ \frac{3\Delta R_B}{\pi^2 R_B^2 C_N C_B R_N} + \frac{1}{2\pi^2 R_N^2 C_N^2} \right\}$$

For the component values adopted in the circuit this is of order $-\delta R_{N/R_N}$ at 1 KHz. and $-3\delta R_{N/R_N}$ at 2 KHz. and can be made negligible by suitable choice of resistor. The effect of changes in C_N is similar, but is probably larger, since the best silvered mica capacitors have temperature coefficients in the range 0-60 ppm/$^{\circ}C$. A maximum coefficient of -1 mb/$^{\circ}C$ may result at zero pressure.

6.1.4. Bridge

In equation 3, ΔR_B is the imbalance in the bridge due to hydrostatic pressure: the bridge is so arranged that the sign of ΔR_B is opposite in adjacent arms, and a differential measurement is made. Temperature effects (e.g. in the diaphragm) which have the same mechanical effect as a pressure change, i.e. introduction of differential strain into the bridge arms, are normally corrected by inserting a small compensating resistor of appropriate temperature coefficient in series with one arm of the bridge. Compensation results in a temperature coefficient of the transducer output sensitivity of less than 0.03%/$^{\circ}C$: a coefficient of $\leqslant 0.03\%$ FRO/$^{\circ}C$ is present in the output at zero pressure.

When the bridge is used in the way described here, this compensation is no longer adequate because some temperature induced changes can be of similar sign in adjacent arms (e.g. temperature coefficient of the wire resistivity).

In a differential amplitude measurement such changes would cancel. For the present system, they do not, and we can write:-

$$\frac{\delta f}{f} \sim \frac{1}{f^2} \cdot \frac{3 \Delta R_B}{\pi^2 R_B{}^2 C_B R_N C_N} \cdot \frac{\delta R_B}{R_B}$$, the effect being

very small at balance.

Direct measurement on one transducer showed the 'common sign' change in R_B to be $\sim$ 300 ppm/^oC. At 2 KHz this would give a coefficient of about -0.6 Hz/^oC or -14 mb/^oC.

The effect of temperature change on C_B is similar to that on R_B, but is much smaller if silvered mica capacitors are used (0-60 ppm/^oC). At most, the temperature coefficient at maximum pressure should not exceed -1.5 mb/^oC.

6.1.5. Stray Impedances

Transformer. The most important stray is the capacity effectively shunting C_B, which may amount to $\sim$ 90 pf. Some difficulty was experienced in measuring the variation of transformer strays with temperature, but results pointed to 1000 ppm/^oC as an upper limit. This would produce an effect no greater than that due to changes in C_B with temperature.

6.1.6. Diodes

The combination of voltage dependent resistance and capacitance is temperature dependent and gives a coefficient at zero pressure (1 KHz) of $\sim$ 5 mb/^oC and at maximum pressure (2KHz) of $\sim$ 11 mb/^oC.

In summary, accurate apportionment of the overall temperature sensitivity between different elements is not easily made, but all the evidence points to the greatest sensitivity being in the bridge itself, even when compensated. The diodes undoubtedly have the second largest sensitivity: rather surprisingly thermal instability in stray impedance seems relatively unimportant. Fig. (5) illustrates the variation in temperature coefficients for several sensors, throughout the pressure range, while Fig. (6) shows the transducer temperature coefficient relative to the sensor temperature coefficient in which it is incorporated. The variation in the behaviour between individual units is a consequence of making the circuit as simple as possible, and electing to make corrections in the subsequent data processing.

6.2. Transient Response to Temperature Change

The discussion of the preceding section assumed that the instrumental response to temperature change is infinitely faster than the change itself. In practice this is not the case: the sensor has a fairly slow transient response, and this can cause significant errors in the pressure measurement if a 'steady state' temperature correction is applied.

Fig. 8 shows the response to a nearly instantaneous temperature change of the sensor mounted in the manner shown in Fig. 7. In this arrangement no attempt has been made to reduce thermal response time. Measurements made on compensated and uncompensated transducers have shown that the initial rise in apparent pressure is contributed by the falling temperature of the transducer diaphragm and strain bridge. Eventually this is offset by a similar, but delayed, fall in temperature of the compensation resistors mounted at the base of the transducer. The sensor electronics increases the overall response time slightly but does not alter the shape of the curves significantly. Fig. 8(a) suggests that the size of the temperature step does not greatly change the nature of the response: in principle a pressure record could therefore be reasonably well corrected retrospectively if the temperature sampling rate were sufficiently high. Fig. 8(b) shows clearly that the 'steady state' value of the temperature coefficient has not been attained 30 minutes after the applied change in temperature: as one might expect, the time constants are not affected by the state of bridge balance, although the magnitude of the 'steady state' temperature coefficient does of course depend on this.

The way in which the dynamic response to temperature affects the accuracy of pressure measurement depends very much, of course, on the temperature changes experienced. Generally, the largest error is incurred when the sensor is subjected to changes of near tidal periodicity. Temperature records obtained to date have shown marked semi diurnal fluctuations, particularly near spring tides, but these have generally not exceeded $0.5^{o}C$ or so. A simplified 'worst-case' calculation in Appendix I shows that at this level, and with the sensor characteristics of Fig. 8(b), thermal response effects are small. However, at some inshore sites (near river estuaries, for example) where temperature changes could be large and periodic, the effects would be serious. A rather different approach to the design of the sensor housing would be required. An otherwise rather difficult design problem could be eased, however, by a reduced working depth requirement.

6.3. Long Term Stability (at Constant Temperature) and its Measurement.

To achieve a stability in pressure measurement of 1 mb in 20 bars over a month requires an overall phase stability in the oscillator of order $1.5\ 10^{-5}$ radians or 0.001^{o} over this period. This means that individual components must have stabilities rather better than:-

	1000 p.p.m.	in L_{ℓ} , R_B
and	2000 p.p.m.	in $R_o + R_p$, L_p
	0.1 pf	in any stray capacity adding to or subtracting from C_B
	50 p.p.m.	in ΔR_B
	5000 p.p.m.	in stability of amplifier gain (closed loop, including diodes)
	50 p.p.m.	in C_B
	50 p.p.m.	in R_N, C_N

It is not really practicable to check the stability of individual circuit elements, excepting, perhaps, the strain gauge bridge. However, quite a large number of different stability measurements have been made on complete sensor units over periods ranging from a few days to three months. These indicate that the stability is within 2 to 3 parts in 10^4 over one month. The instabilities in the electronics and strain gauge transducer are thought to be of roughly the same order.

Since achievement of good stability was regarded as important, quite a lot of thought has had to be given to ways of generating nearly constant operational pressures and temperatures in the laboratory, and of measuring them. The need to determine long term stability to within 1 part in 2.10^4 calls for the measurement of pressure to about 10^{-4} bars and temperature to about $0.02^{o}C$. Ideally the system should also be capable of fine adjustment to within these limits, to allow readings to be made under directly comparable conditions.

To satisfy these requirements a servo controlled 0-20 bar pressure tank with thermostatic temperature control has been developed. The pressure measurement and control reference is a Texas Instruments quartz bourdon capsule whose calibration has been checked at approximately 12 monthly intervals against an NPL-calibrated dead-weight tester. The facility has been an invaluable aid to

the sensor test programme generally, although it has so far been used rather less for long term stability testing than was originally intended. This is due in part to the rather conflicting aims of trying to develop a complex piece of equipment and use it routinely at the same time: the tank also affords a good means of calibrating sensors, and an extensive programme of tide measurements has reduced its availability for long term occupation. A third and exasperating reason has been the relatively high incidence of mains power failures over the past three years; of necessity these trip the safety interlocks on the system, which then automatically closes down.

Another method of assessing long term instability is to filter out the tides from corrected sea bed pressure records obtained using the sensors and to examine the residual time series. One can deduce a rough 'upper limit' for instrumental drift in this way: an accurate assessment is not possible because no reference is available, and because there are changes in mean sea level which obscure small amounts of instrumental drift. An example is given in Fig. 9 where five simultaneous filtered pressure records are shown. These were derived from tide records obtained from a line of positions N.W. of Scotland in August 1971. 2(a) and (b) are records from two independent strain gauge sensors mounted on the same gauge. Records 3 and 5 were taken from gauges equipped with the older-type variable capacitance transducer which were sited at distances away of 100 and 300 km, respectively. Record 4 is a shorter record obtained using a capacitance transducer on a tide gauge 200 km distant. The records contain some remarkably well correlated fluctuations, which can only represent real changes in mean sea level. But also noticeable are the steady drifts of the sensors relative to one another, although these are considerably less in the case of the strain gauge sensors. Here, the relative drift is seen to be < 7 cm in 30 days. The difficulty of obtaining even a rough estimate of absolute instrumental drift, especially from a single record, is evident.

Two deployments a few months later produced the large apparent drifts in mean pressure shown in Fig. 10., and these show that unforeseen problems can arise even after an instrument has been checked carefully in the laboratory beforehand. In this series of deployments the strain gauge diaphragm was isolated from the sea by filling the orifice with oil, using a very thin flexible outer diaphragm to communicate the pressure changes to the transducer. During calibration and testing the sensor operated faultlessly, but on immersion in the sea some form of chemical attack took place and the diaphragm became porous and distorted. During the month the oil slowly leaked away and the

sensor output exhibited a large instability in mean pressure. The principal tide data were recovered with little loss of accuracy, but the longer period information was irrecoverable.

6.4. Pressure Hysteresis

This parameter is surprisingly difficult to measure accurately. A full range 20 bar pressure change produces a typical temperature change of 0.17°C in the working fluid (Shell Tellus oil 11) in contact with the transducer diaphragm due to adiabatic expansion and compression. This generates an immediate error in the sensor output due to the thermal response of the diaphragm (section 6.2), and the sensor therefore has to be allowed to stabilize its temperature. The measurement can be done either by immersing the entire sensor in the pressure tank, or by connecting a pressure line to the transducer orifice and using a dead weight tester for the measurement. The temperature control system for the pressure tank has rather a long time constant and the dead weight tester was used instead. By allowing the transducer 15 minutes to stabilize at each pressure change, and taking care that the dead weight tester (D.W.T.) was in reasonably constant temperature surroundings, (D.W.T. temperature coefficient = 0.0015%/°C of measured pressure) reproducible results were obtained. The maximum amount of hysteresis, 3 mbars, was observed at mid range.

6.5. Thermal Hysteresis

This was checked at a constant pressure of 20 bars. Sensors were cycled between 4 and 18°C, measurements being made at 3 or 4 points in each direction. Sufficient time was allowed at each point for the sensor temperature to stabilize. The maximum amount of hysteresis was less than 4 mbars.

6.6. Dynamic Pressure Effects.

Whenever a pressure sensor is placed in a moving fluid it will, in general, measure a dynamic pressure component in addition to the static head. The magnitude of the dynamic pressure is $\frac{1}{2} c \rho v^2$, where c is a coefficient depending on the shape of the sensor, its mounting system, and on the direction of flow; it has a maximum value of ± 1.

A series of measurements were made of dynamic pressures on the cylindrical sensor housing (Fig.7) when towed at various speeds along the IOS wave tank at constant depth. These are shown in Fig. 11. The magnitude of the errors can clearly be quite large if an unsuitable housing is used. (Note the sudden change in pressure as the top of the housing is tilted through the horizontal;

this is due to a sudden change in the flow seperation at the leading edge of the casing and a consequent change in flow across the orifice.) A simple fairing mounted around the housing improves the situation.

Hitherto the errors incurred have been small because tidal currents have generally been of order 1 knot or less, and at the working depths (> 120 metres) wave induced dynamic pressures have been negligible.

6.7. Supply Voltage Sensitivity

Fig.12 illustrates the error introduced by variations in the positive and/or negative supply voltages at 1 bar and 20 bars pressure.

7. OPERATIONAL PERFORMANCE

The first use of these sensors at sea was in August 1971 and by December 1973 230 days of useful data had been obtained from eight tide gauge deployments. An early assessment of the performance of the complete instrument has been given by Collar and Cartwright.[6]

More recently, in November and December 1973, the SCOR Working Group on Tides of the Open Sea (W.G.27) held an intercomparison exercise in which tide capsules developed by research groups in a number of countries were laid at two sites in the Bay of Biscay. One of the sites was on the Continental Shelf at a depth of 170 metres: the second site was in the deeper water to the west (2200 metres). The gauge contributed by the Wormley group was laid at the first site (170 metres depth) and carried a strain gauge sensor as well as one of the older variable capacitance sensors. The pressure record obtained from the strain gauge sensor is shown in Fig.13 (centre panel) together with the temperature record (top). Note the appreciable fluctuation in temperature at tidal frequencies due to internal wave activity. The two records shown in the bottom panel are from the strain gauge (wavy record) and the variable capacitance sensor (smooth curve), and are of mean sea bed pressure after removal of the tides by filtering during computer processing. In order to accommodate the very much greater instrumental drift of the capacitance sensor the scale on the left hand axis has been reduced by a factor of 25 over that for the right hand axis, which refers to the wavy strain gauge record. Although this is not apparent in Fig.13, replotting the smooth curve on a larger scale shows the presence of fluctuations similar to those registered by the strain gauge. They represent real pressure fluctuations and are not instrumental instabilities.

A detailed description of the results of the intercomparison exercise is given in the Working Group's Report[7]; table 2 contains an extract from these and shows the amplitudes and phases of the major semi-diurnal constituents obtained from the strain gauge and variable capacitance sensor records. Also shown for comparison are the corresponding values obtained from a Hewlett Packard Quartz sensor and a Vibrotron sensor, which were mounted on another IOS gauge laid independently at the same site. In this particular aspect, the performance of the strain gauge sensor was comparable to that of the more expensive sensors.

TABLE 2:

Amplitudes and phases of major semi diurnal constituents extracted from Continental Shelf tide records produced by different sensors during the SCOR Intercalibration Exercise, November 1973. (Depth 170 metres).

Constituent	Amp / Phase ^{o}	Hewlett Packard Quartz	Vibrotron	Capacitance Plate	Strain Gauge
M_2	H	130.9	130.9	129.3	130.2
	G^{o}	103.3	103.4	103.4	103.5
S_2	H	44	43.3	43.2	43.6
	G^{o}	136.6	136.3	135.8	135.9
N_2	H	27.4	26.8	26.9	27.1
	G^{o}	84.3	84.8	84.3	84.3
K_2	H	12	11.8	11.7	11.9
	G^{o}	139.0	139.0	138.4	138.5

The technique has now been extended to the measurement of deep sea tides and of temperature, and records of good quality have been obtained at depths of 1200 and 2200 metres.[8] Good agreement has emerged from a comparison[7] of the tidal constants derived from a deep strain gauge record obtained at the SCOR site in March 1974 and those derived from two Hewlett Packard crystals and a Filloux bourdon tube during the SCOR exercise itself.

8. CONCLUSION

The suitability of the strain gauge sensors for measurements of the principal tides on the Continental Shelf has been clearly demonstrated. Furthermore they are sufficiently stable to permit their use in investigations of changes of several days' periodicity. The limitations that have been encountered are principally those of excessive transient response to large

temperature changes, and response to dynamic pressures induced by water flow; these will probably cause significant errors in very shallow water. Both limitations are shared to a greater or lesser extent by all pressure sensors, although the mechanical design of the present sensor can be changed to improve the performance of the sensor in both respects.

The major advantage of the sensors lies, we believe, in their simplicity and hence comparatively low cost. This is an important factor in designing equipment which may well be left unattended in the middle of well-trawled fishing grounds. We reiterate our belief that as far as possible equipment should be designed for simplicity leaving corrections for unwanted secondary sensitivities to be handled, wherever practicable, in subsequent data processing, rather than attempt to remove these at source in a more complex equipment.

9. ACKNOWLEDGEMENTS

We are grateful for the help of a number of colleagues at Wormley at different times during the work on the sensors. In particular, Mr. R.E. Kirk carried out the measurements in the towing tank as part of a wider study of dynamic pressure effects being conducted by Dr. R.M. Carson: Dr. B.S. McCartney made some very helpful comments during the preparation of the manuscript.

REFERENCES

1. Skinner, L.M. and Rae, J.B. (1974) - The use of pressure sensors for tidal and water level measurements.

   Proceedings of a European Symposium on Offshore Data Acquisition Systems. 16th-18th September 1974. Society for Underwater Technology, London, pp 185-198.

2. Collar, P.G. and Spencer, R. (1970) - A digitally recording offshore tide gauge.

   Proceedings of a Conference on Electronic Engineering in Ocean Technology. 21st-24th September 1970. (Conference Proceedings No. 19). IERE, London, pp 341-352.

3. Snodgrass, F.E. (1968) - Deep sea instrument capsule. Science 162, 78-87.

4. Stastny, G.F. and Butts, R.S. (1953) - Strain gauge remote metering Tele-tech and electronic industries, March 1953, 73-75, 175-176.

5. Hamon, B.V. and Brown, N.L. (1958) - A temperature-chlorinity-depth recorder for use at sea. J. Scientific Instruments 35, 452-458.

6. Collar, P.G. and Cartwright, D.E. (1972) - Open sea tidal measurements near the edge of the Northwest European Continental shelf. Deep-Sea Research, 19, 2, 673-689.

7. UNESCO Technical papers in Marine Science. An intercomparison of open sea tidal pressure sensors, sponsored by SCOR, IAPSO and UNESCO. SCOR Working Group 27 "Tides of the open sea". (To be published).

8. Spencer, R. and Gwilliam, T.J.P. (1974) - A sea-bed capsule for measuring tidal pressure variations at depths up to 4000 metres.

   Proceedings of IEEE. International Conference on Engineering in the Ocean Environment - Ocean 74.
   Institute of Electrical and Electronic Engineers, New York Vol I, pp 339-343.

APPENDIX 1 : An order of magnitude estimate of the error incurred in neglecting the transient temperature sensitivity of a pressure sensor.

In practice the nature of the temperature and pressure changes and the response to them is far too complex for the errors to be evaluated by simple analytical means. Nevertheless by making some simplifying assumptions a useful order-of-magnitude limit for the errors can be obtained. These assumptions are:

1. Since the effect is likely to be most serious when the temperature changes encountered are of tidal periodicity we assume a sinusoidal temperature variation of constant amplitude (worst case). Changes in sea bed pressure due to tides are assumed to have negligible influence on transient temperature response.

2. The system is assumed to be linear. i.e. the apparent change in pressure shown by the sensor in response to this periodic temperature change can be deduced from laboratory measurements of its response to a step change in temperature.

3. If the sensor is subjected to a unit step in temperature at $t=_o$ then the apparent change in pressure can be described approximately as a function of time by

$$F_o(t) = A\ (1-e^{-t/\tau_1}) - B\ (1-e^{-(t-t_o)/\tau_2}).\ H(t-t_o)$$

and $H(t) = o$ for $t < o$

$= 1$ for $t > o$

where t_o is defined in fig.14.

$F_i(t) =$ o for $t < o$, 1 for $t > o$

This form of approximation is assumed for simplicity and is not an attempt to represent the physical process of heat transfer through the sensor.

A measured response derived from fig.8b, and an approximation to it, are shown in fig.14.

The values of the constants used are:

$A = 18$ mbar/^oC : $t_o = 300$ sec.

$B = 11.5$ mbar/^oC : $\tau_1 = 120$ sec. : $\tau_2 = 800$ sec.

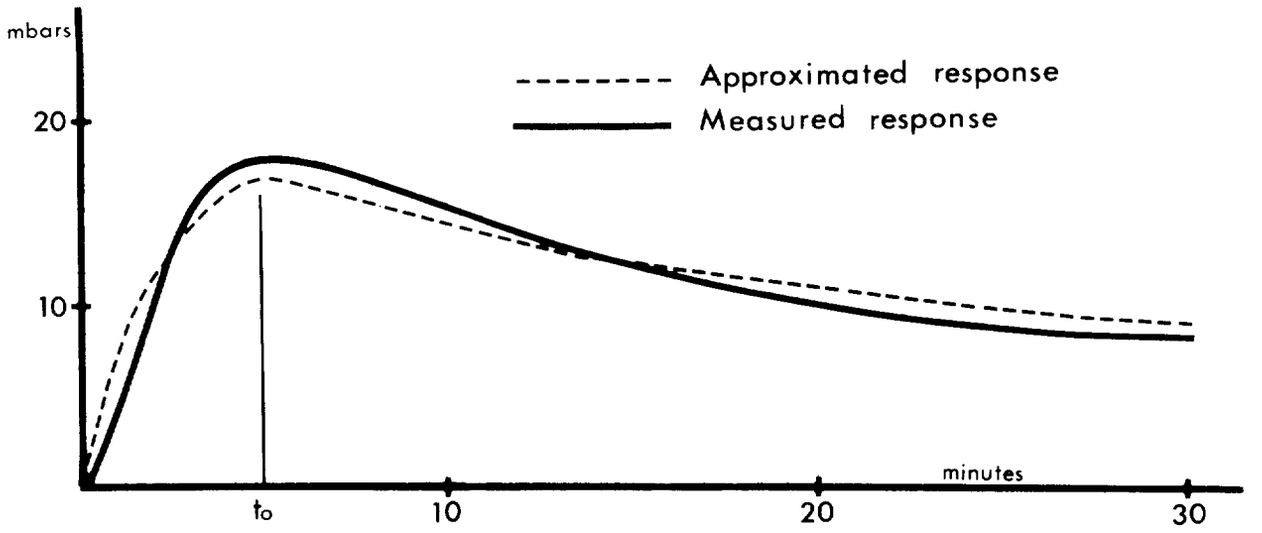

Fig.14 Measured and approximated response of the pressure sensor to a unit step in temperature.

We can now use the Laplace transformation and express the transform of the response of the system to the temperature step as

$$\mathcal{L}(R) = p\left(\frac{A}{p} - \frac{A}{p+1/\tau_1} - e^{-pt_o}\left(\frac{B}{p} - \frac{B}{p+1/\tau_2}\right)\right)$$

where p is defined by

$$\mathcal{L}f(t) = \int_o^\infty e^{-pt} f(t).\ dt.$$

If, in use, the sensor experiences a sinusoidal change in temperature $\Delta T \cos\omega t$, then in steady state conditions the transform of the pressure error is:

$$\mathcal{L}(\Delta P) = p\Delta T\left(\left(\frac{A}{p} - \frac{A}{p+1/\tau_1}\right) - e^{-pt_o}\left(\frac{B}{p} - \frac{B}{p+1/\tau_2}\right)\right) \cdot \frac{p}{p^2+\omega^2}$$

By expanding in partial fractions, and taking the inverse transforms,

$$\Delta P(t) = p\Delta T\left(\frac{A}{(1+\omega^2\tau_1^2)^{\frac{1}{2}}}\cos(\omega t-\phi_1) - \frac{Ae^{-t/\tau_1}}{(1+\omega^2\tau_1^2)} - H(t-t_o)\left(\frac{B}{(1+\omega^2\tau_1^2)^{\frac{1}{2}}}\cdot\right.\right.$$

$$\left.\left.\cdot\cos(\omega(t-t_o)-\phi_2) - \frac{Be^{-(t-to)/\tau_2}}{(1+\omega^2\tau_2^2)^{\frac{1}{2}}}\right)\right)$$

where $\phi_1 = \tan^{-1}\omega\tau_1$ and $\phi_2 = \tan^{-1}\omega\tau_2$

For $t \gg t_o$, i.e. in steady state conditions,

$$\Delta P = \Delta T \frac{A}{(1+\omega^2\tau_1^2)^{\frac{1}{2}}} \cos(\omega t - \phi_1) - \frac{B}{(1+\omega^2\tau_2^2)^{\frac{1}{2}}} \cos(\omega(t-t_o) - \phi_2)$$

$$= K\Delta T \cos(\omega t - \theta)$$

where $$\theta = \tan^{-1} \frac{a\sin\phi_1 - b\sin(\phi_2 + \omega t_o)}{a\cos\phi_1 - b\cos(\phi_2 + \omega t_o)}$$

$$K = (a^2 + b^2 - 2ab\cos(\phi_1 - \phi_2 - \omega t_o))^{\frac{1}{2}}$$

and $$a = \frac{A}{(1+\omega^2\tau_1^2)^{\frac{1}{2}}}, \quad b = \frac{B}{(1+\omega^2\tau_2^2)^{\frac{1}{2}}}$$

Whenever regular temperature changes have occurred in the tide pressure records obtained so far they have had a period of about 12 hours and have tended to reach maximum amplitude ($\sim 0.25^oC$) near spring tides, disappearing altogether at other times during the monthly cycle. Fig.13 is fairly typical in this respect. In order to make a rough estimate of the maximum likely error due to thermal transient effects we assume that temperature changes are of constant amplitude ($\Delta T = 0.25^oC$) throughout the record and have the exact periodicity of a composite semi-diurnal tide.

If the 'true' pressure component is $P_o \cos\omega_o t$, the output of the pressure sensor can be written as:

$$P_{app} \cos(\omega_o t + \gamma) = P_o \cos\omega_o t + K\Delta T \cos(\omega_o t - \theta)$$

Referring to fig.14, we see that in the present case, values of $\omega\tau_1$, $\omega\tau_2$ are sufficiently small that

$$K\Delta T \simeq (A-B)\Delta T = 6.5 \times 0.25 = 1.6 \text{ mbar}$$

and $$\theta \simeq \frac{A\phi_1 - B(\phi_2 + \omega t_o)}{A-B} \approx -13^o$$

Taking a typical value for P_o as 150 mbar, we then find that in the absence of any temperature correction the apparent semi diurnal amplitude P_{app} is too large by about 2 mbar (1.5%) and has also a phase angle (lead) error of 0.14^o.

If, now, the transient temperature response is ignored but a temperature correction is made on the basis of an equilibrium coefficient A-B ($\sim$K) then after correction the apparent pressure becomes: $P_{app}\cos(\omega_o t + \delta) \equiv$ $P_o \cos\omega_o t + K\Delta T \cos(\omega_o t-\theta) - K\Delta T \cos\omega_o t$. On evaluation this shows a reduction in the amplitude error to about 0.02%, but a phase error of $\sim 0.14^o$ remains.

The discrepancies obtained in practice between different sensors measuring the same tidal pressure changes (Table 2) helps to put this rather crude 'worst case' estimate of phase error into perspective. We conclude that neglect of transient temperature effects is probably justified in the conditions encountered so far. However, if response times are longer relative to the tidal period of interest or periodic temperature changes are much greater, then temperature correction may need to take the thermal response time of the sensor into account.

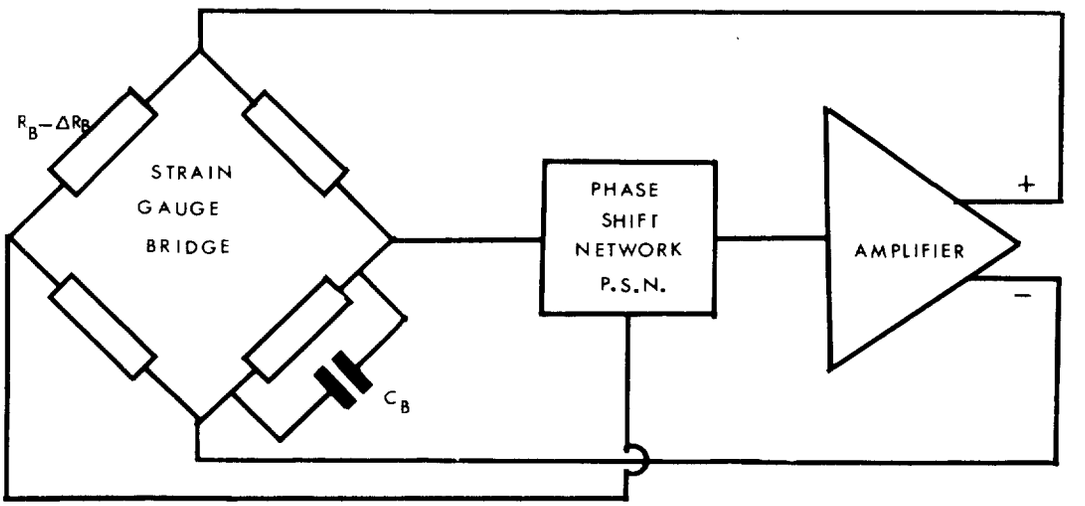

Fig. 1. Block schematic showing principal components of oscillator

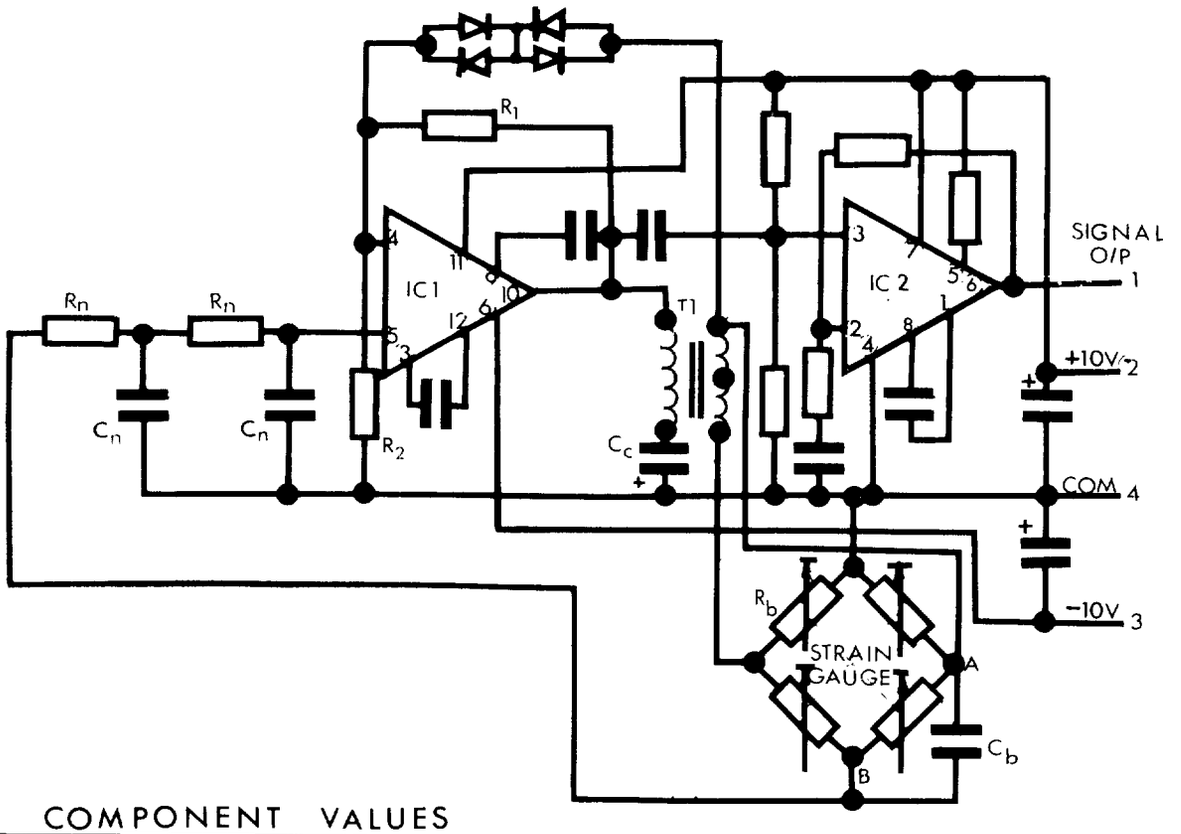

TYPICAL COMPONENT VALUES

R_n = 10 K Ω	R_1 = 680 K Ω
C_n = 0·015 μF	R_2 = 560 Ω
R_b = 1K Ω	C_c = 100 μF
C_b = 2000 pF	

R_b = 4 Ω at F.R.O.

Fig. 2. Pressure sensor circuit diagram

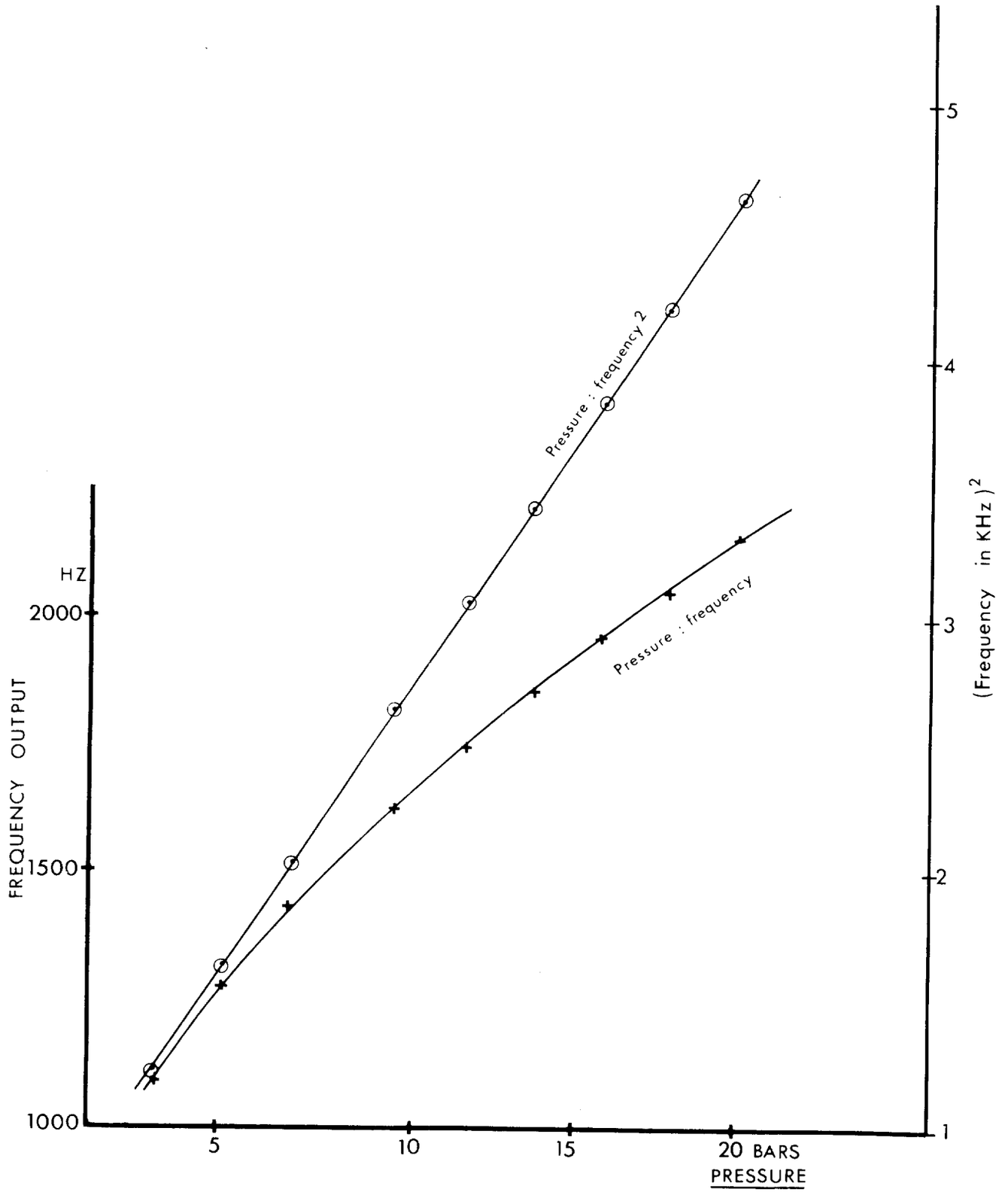

Fig.3 PRESSURE - FREQUENCY characteristic of pressure sensor.

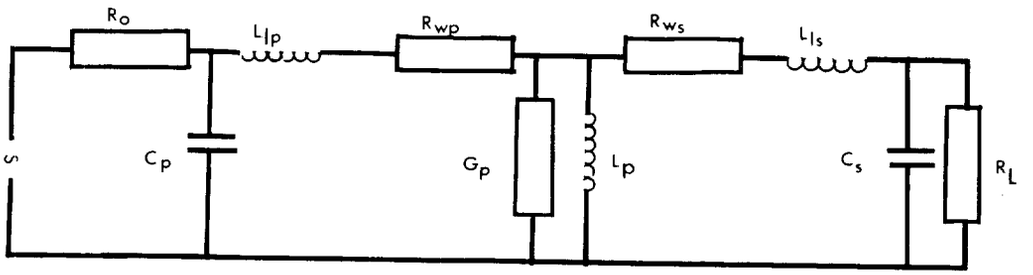

Fig. 4a

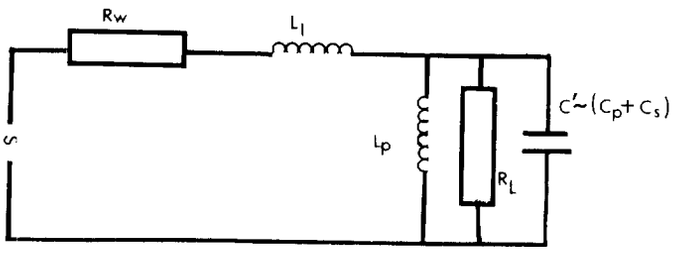

Where $L_l \sim L_{lp} + L_{ls}$ (for $n = 1$)

$R_w \sim R_o + R_{wp}$

$R_{ws} \ll R_l$

Fig. 4b

Note: interwinding capacities not shown.

L_l	-	Leakage inductance referred to primary	$\sim$ 1·5 mH.
R_o	-	Generator output impedance)	$\sim$ 4 Ohms
R_w	-	Winding resistance ($R_{wp} \simeq R_{ws}$)	$\sim$ 10 Ohms
G_p	-	Conductance (Core loss)	$\sim$ 0·0005 mhos
L_p	-	Magnetising inductance	$\sim$ 850 mH.
R_L	-	Load (assumed resistive)	$<$ 1000 Ohms
C'	-	Lumped self capacity	$<$ 500 pf
n	-	Turns ratio (primary : secondary)	$\sim$ 1

Fig. 4. Transformer equivalent circuit

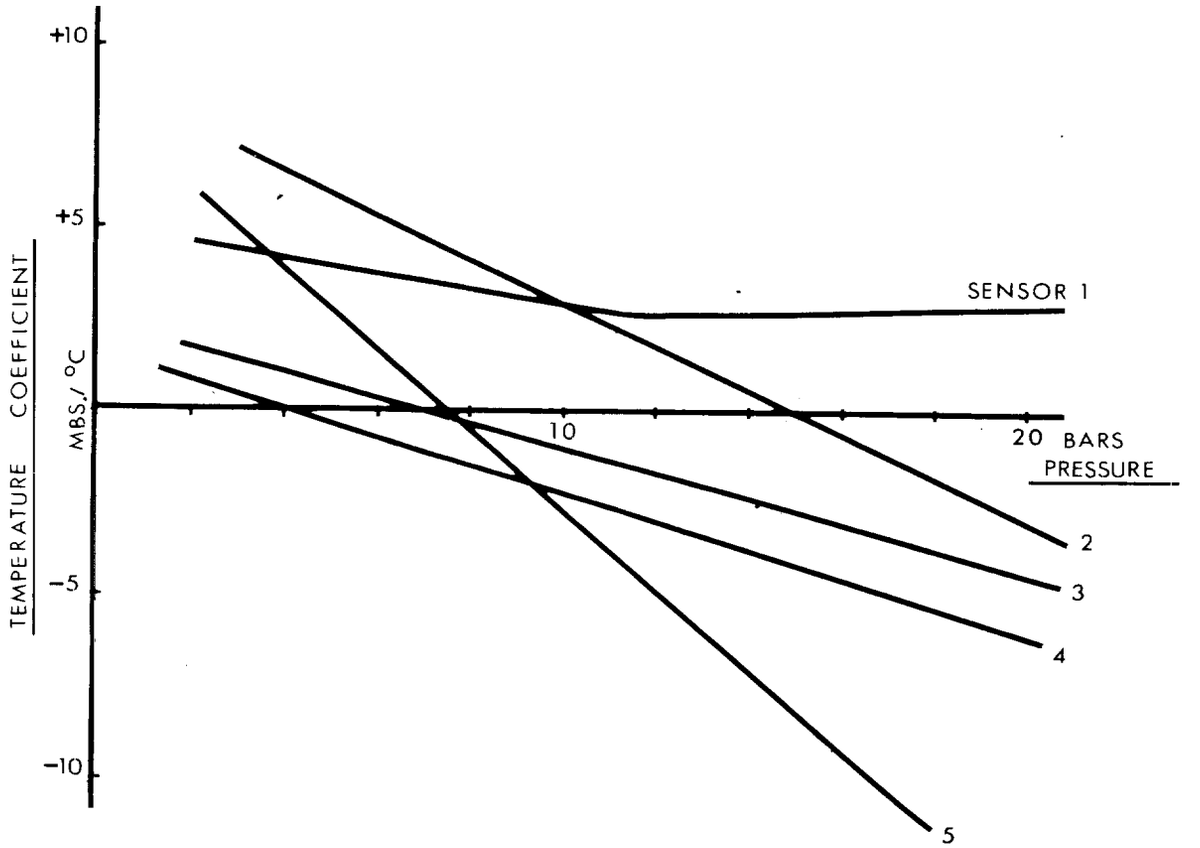

Fig. 5. Variation of temperature coefficient with pressure change for five sensor units

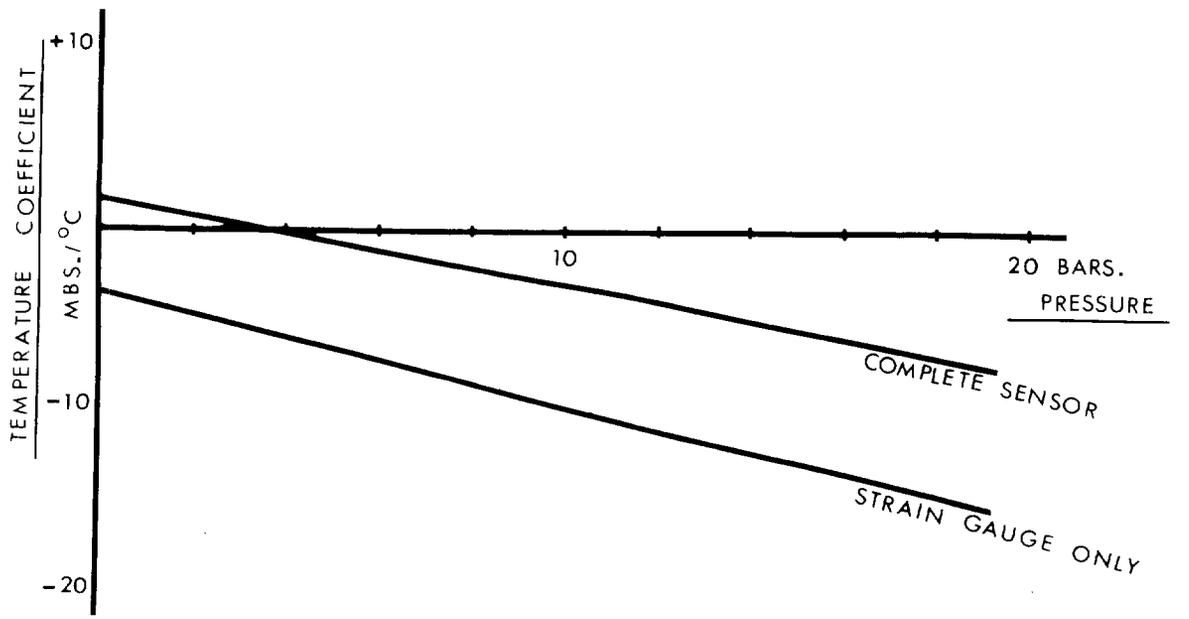

Fig. 6. Showing relative magnitudes of coefficient for a strain gauge and complete sensor from measurements obtained independently

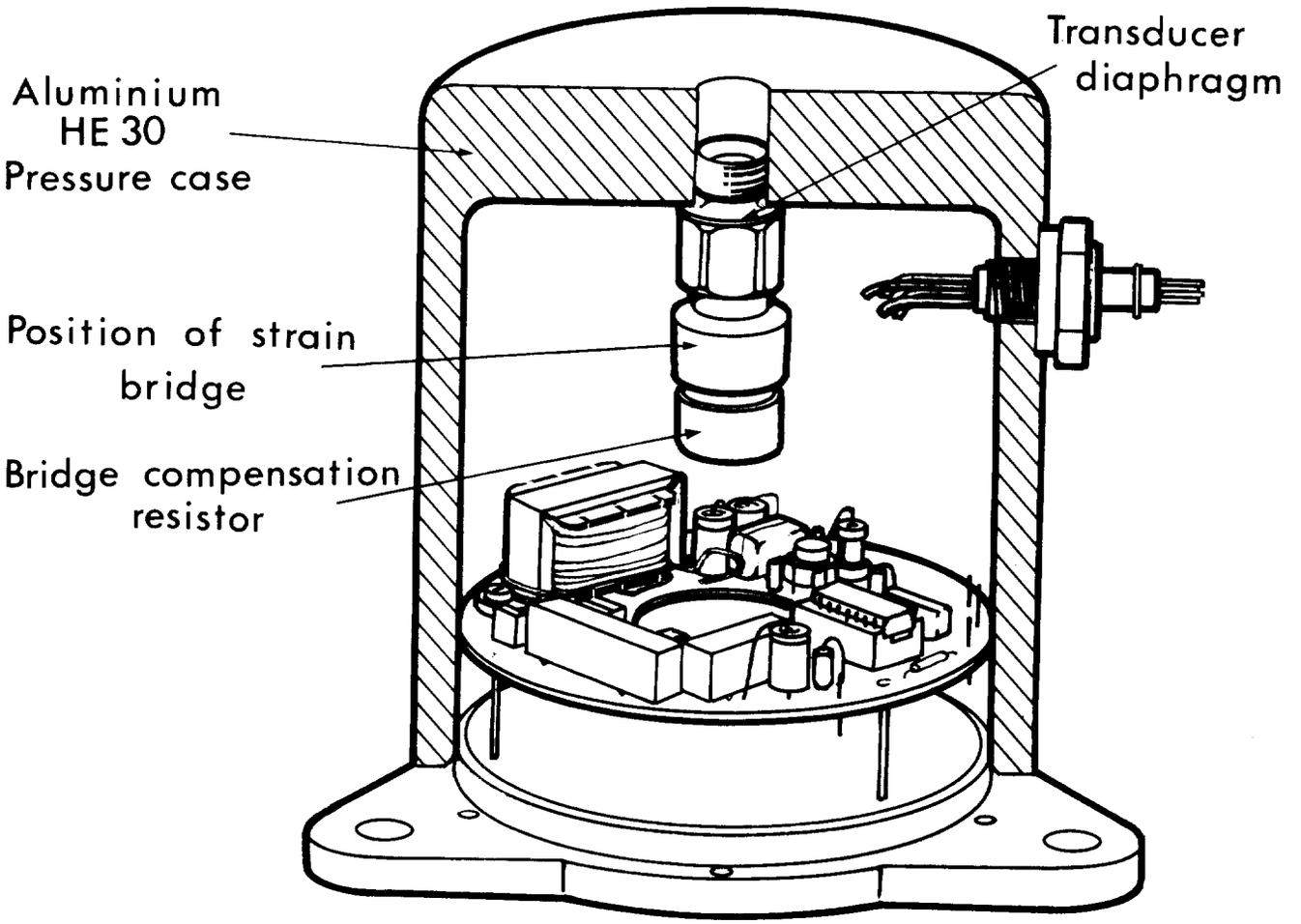

Fig.7. General arrangement of strain gauge pressure sensor. (No attempt has been made with this particular housing, to minimize thermal transient response or dynamic pressure effect)

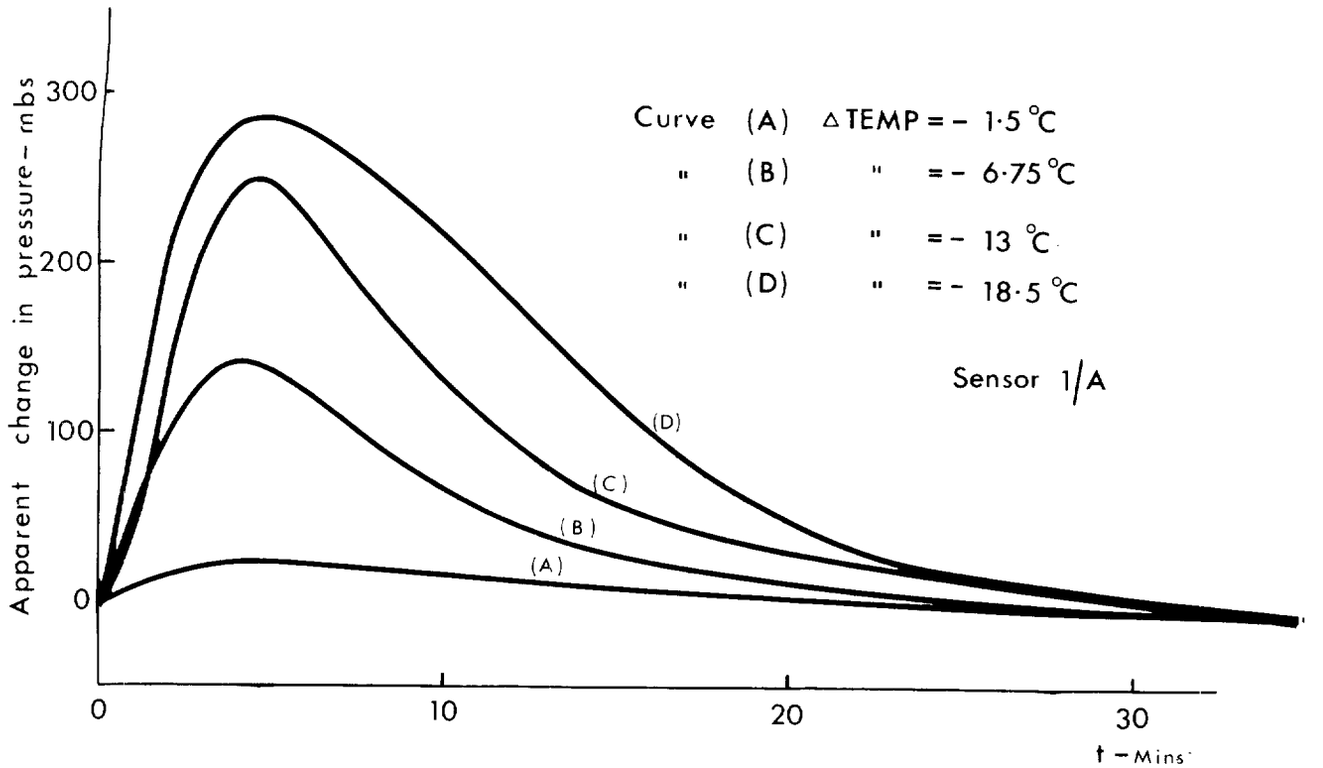

Fig. 8 (a) Transient response of pressure sensor, at atmospheric pressure, to negative steps in temperature at time t = 0

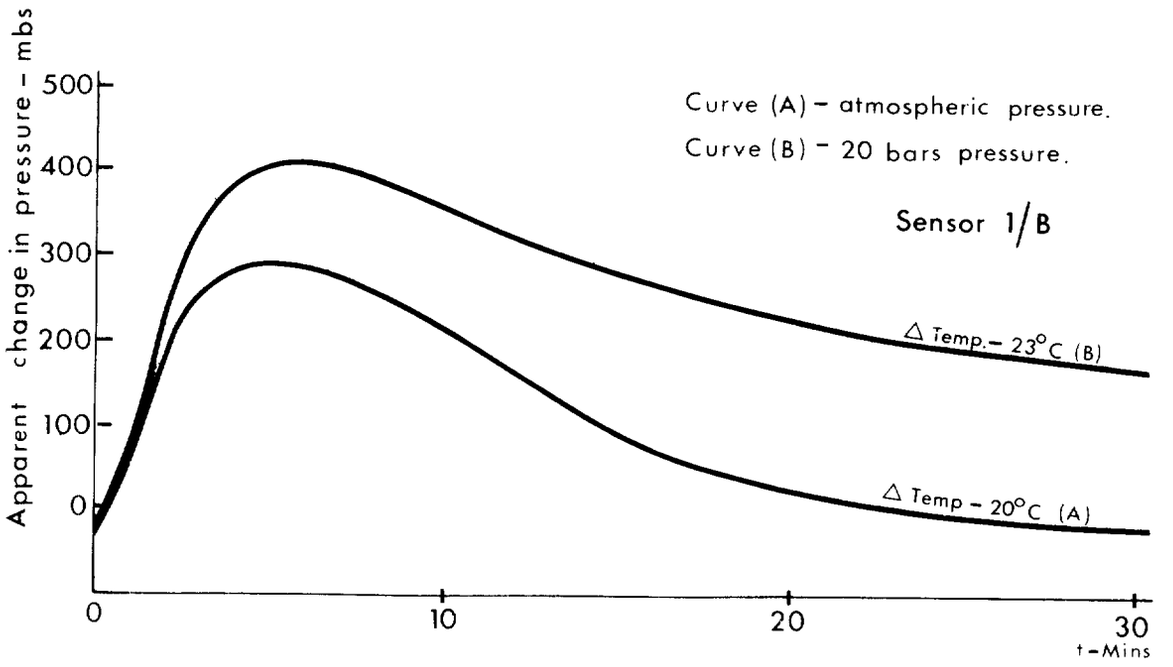

Fig. 8(b). Transient response of pressure sensor to a negative step in temperature at time t = 0

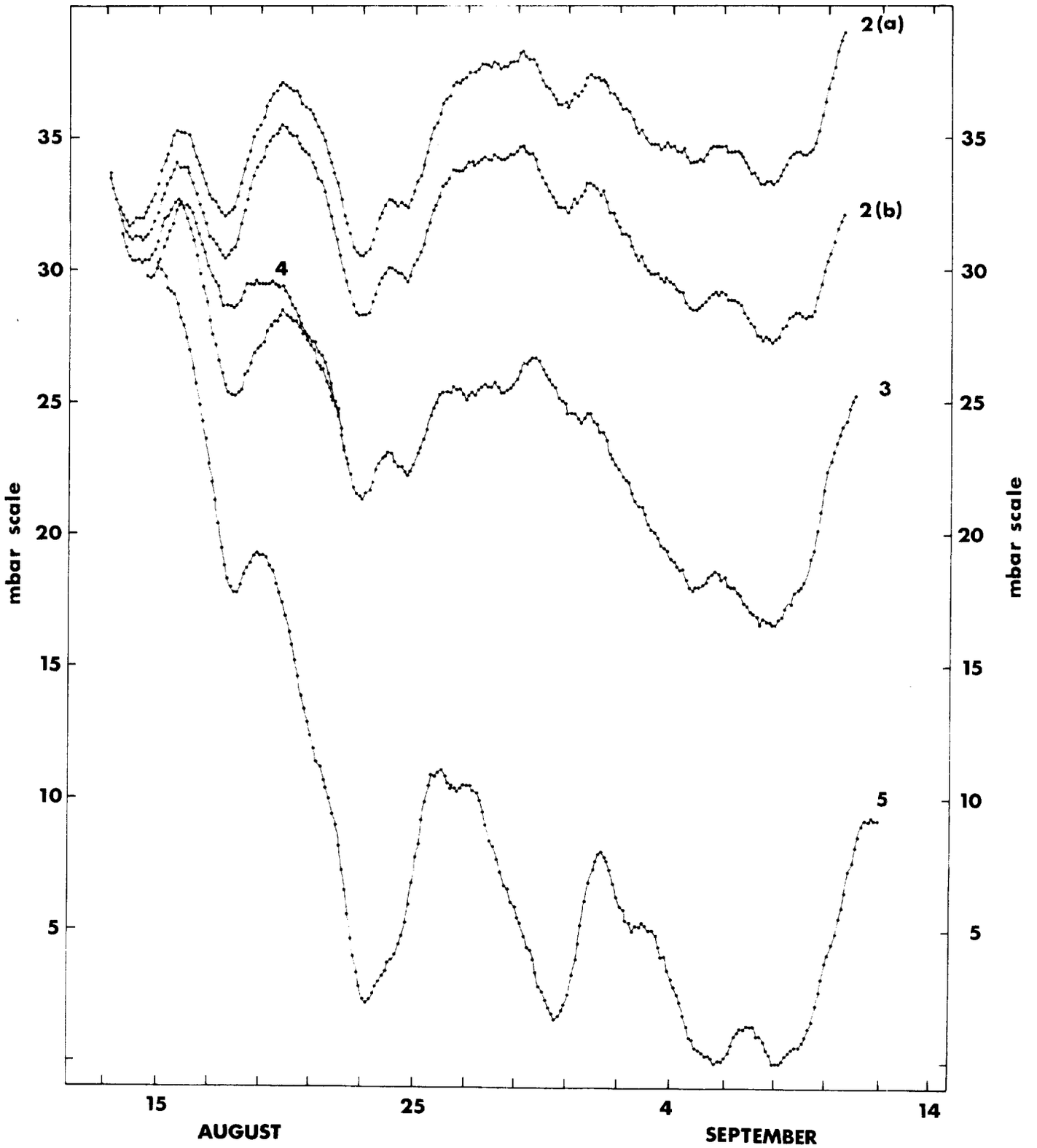

Fig. 9 Slow simultaneous sea bed pressure changes and instrumental drifts after removal of tides by filtering. Positions 2 to 5 form a sequence of stations with separation 100 km.

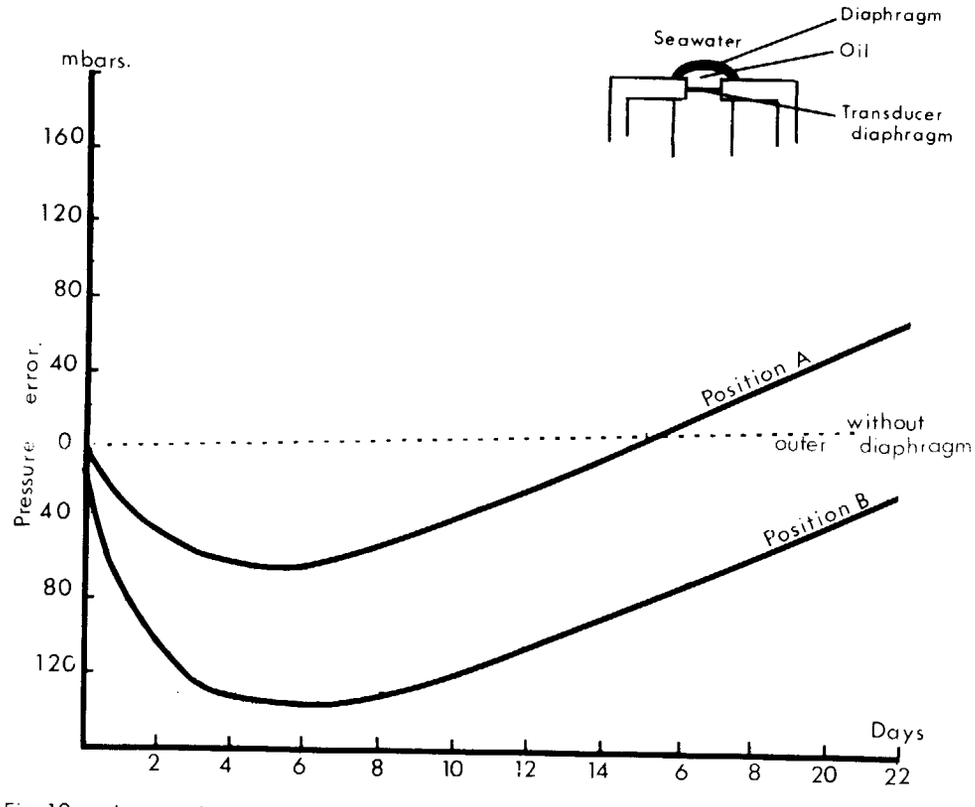

Fig. 10. Large instrumental drift introduced by slow failure of outer diaphragm of sensor. Note that real sea bed pressure changes are completely masked.

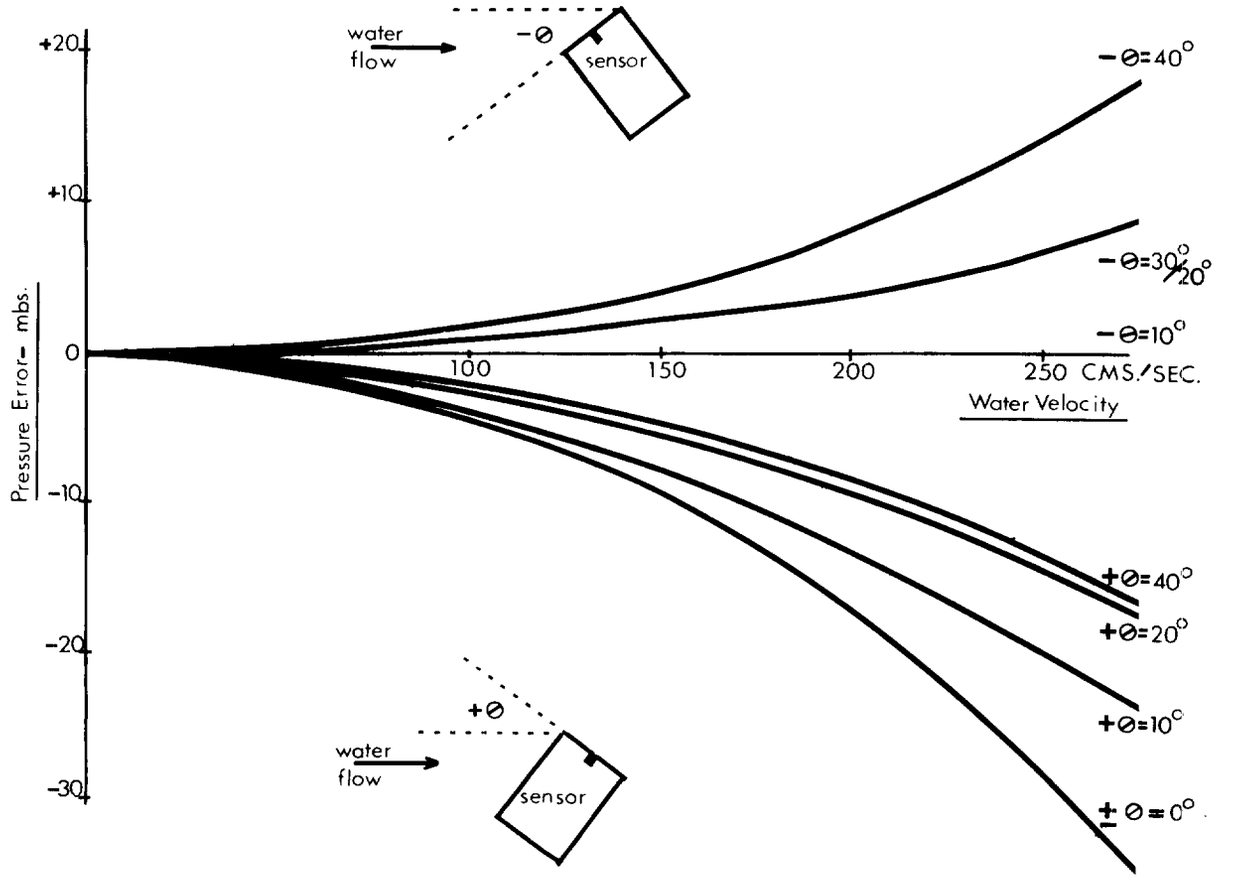

Fig.11. Experimental results showing pressure errors occurring with positional changes of the sensor housing when placed in a water tank and towed at velocities up to 250cms/sec.

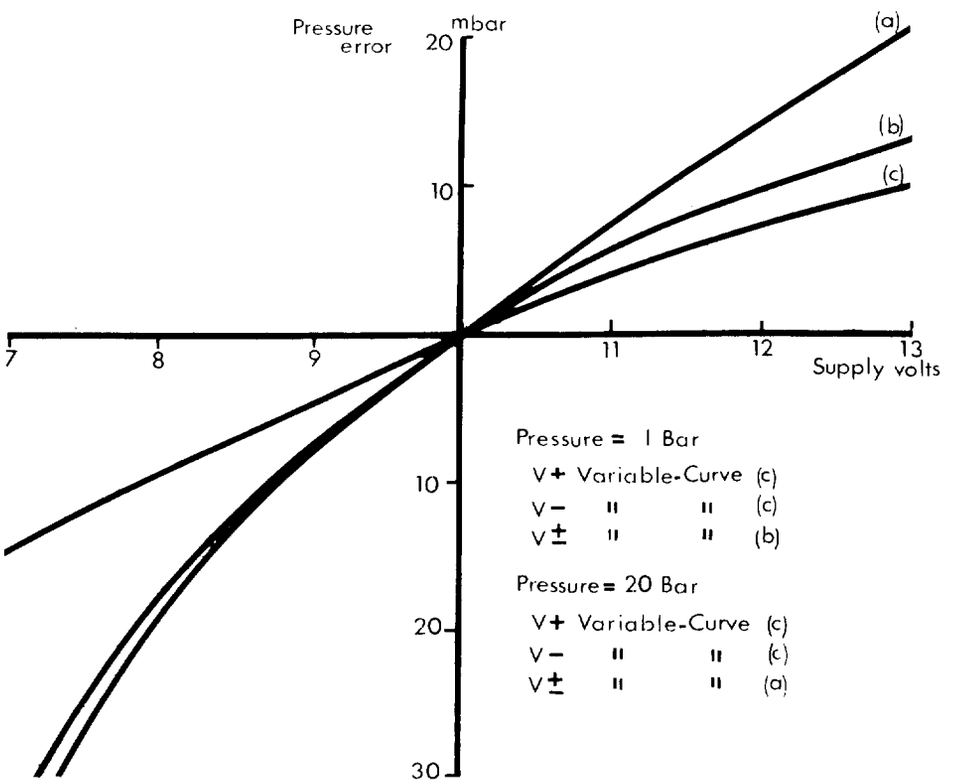

Fig.12 Variation of sensor output with change in supply voltages.

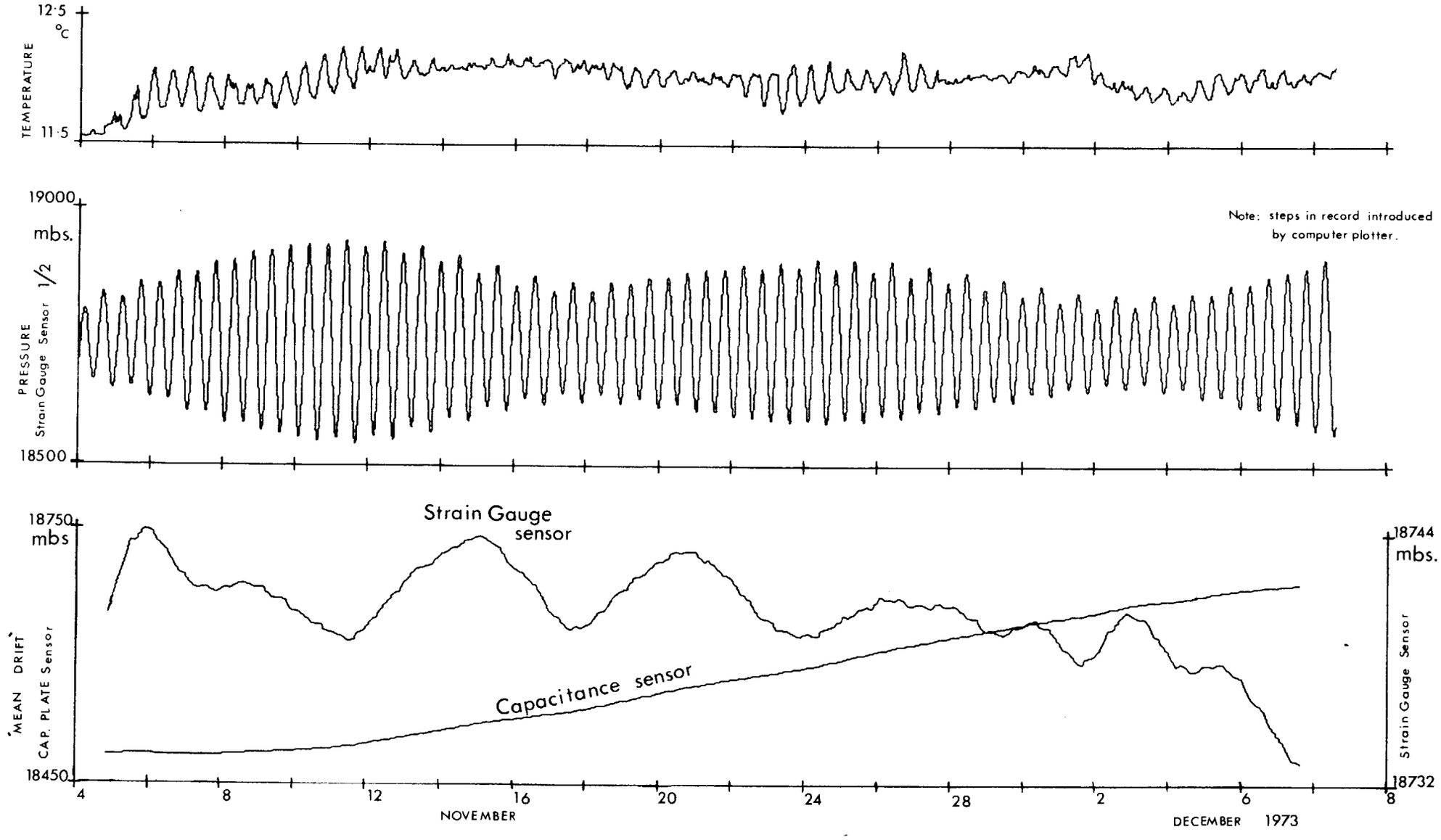

Fig. 13. Pressure and temperature data collected on the S.C.O.R. W.G. 27 Intercalibration exercise using the I.O.S. Wormley tide gauge system.